

A coupled field-circuit model of a 5-phase permanent magnet tubular linear motor*

BRONISŁAW TOMCZUK, ANDRZEJ WAINDOK

*Department of Industrial Electrical Engineering, Opole University of Technology
Luboszycka 7, 45-036 Opole, Poland*

e-mail: b.tomczuk@po.opole.pl

(Received: 02.07.2010, revised: 19.11.2010)

Abstract: A method for modeling of the dynamics characteristics for a 5-phase permanent magnet tubular linear motor (PMTLM) is presented. Its electromagnetic nonlinear field analysis with finite element method (FEM) has been coupled with the circuit model. The calculation model includes the equations for electrical circuits and mechanical quantities as well. They have been obtained using Lagrange's method. The calculated and measured waves of the mover position have been compared for several values of the excitation current. This comparison yields a good agreement. Presented calculation model is very useful in designing and optimization of the PMTLM and in the calculation of the parameters for the control algorithms intended for such a type of actuators.

Key words: permanent magnet linear synchronous motors (PMLSM), field-circuit method, simulation of the transients, control parameters

1. Introduction

The permanent magnet linear motors (PMLM) which are of great significance among electromagnetic accelerators have focused strongly attention in recent years. They provide an alternative against pneumatic or hydraulic drives in many applications involving high-speed or/and high precision motion control [1, 2]. The PMLM's have usually large air-gap, high force density, good dynamic properties, low losses and quite simple structure. Thus, they are used in high-performance drive systems and servo applications [3-5]. The growing demands for better and better PMLM's parameters involve the need for mathematical modelling of the motors transients. For example, in this work we present the field-circuit method application for analysis of modern linear actuator transients.

The analysed actuator, called permanent magnet tubular linear motor, belongs to the group of linear synchronous machines [6]. Due to advantageous to the construction magnetic flux distribution, it is marked by the higher force/weight ratio comparing with other linear motors

*This is extended version of a paper which was presented at the 21st *Symposium on Electromagnetic Phenomena in Nonlinear Circuits*, Essen-Dortmund, 29.06-02.07, 2010.

(e.g. flat ones). There is high density of the magnetic flux lines which are directed towards the main axis of the motor symmetry. The flux density determines the force along the movement direction (Fig. 1).

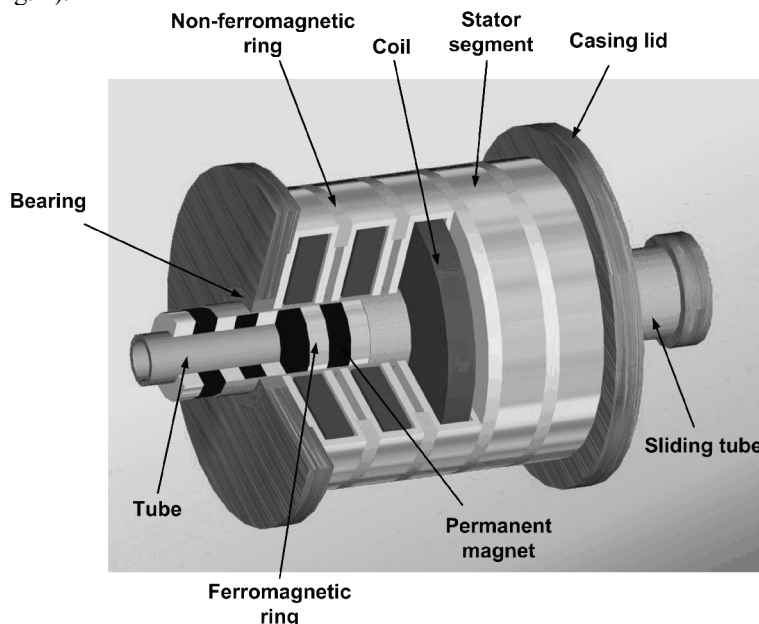


Fig. 1. View of the motor with stator cutting out

Linear motors have been widely studied with the electric circuit theory [6, 7]. The permanent magnet (PM) motors were widely considered, e.g. in [8-10]. However, the transients of the multiphase constructions have not been often investigated. Most of the linear actuators have no more than three phases. The actuators with four or more phases are investigated occasionally. Thus, at the Opole University of Technology, in Department of Industrial Electrical Engineering (DIEE), a 5-phase tubular actuator has been developed (Fig. 1). It was patented by Tomczuk and Waindok [11]. One of the unique features of the actuator is the segmented construction of the stator, which results in very small values of the mutual inductance.

One of the disadvantages of the permanent magnet linear synchronous motors (PMLSM) is the cogging (detent) force, which arises from the interaction of the permanent magnets and the ferromagnetic core. The cogging forces play down the motor performances and generate mechanical vibration, acoustic noise and velocity oscillations as well. Thus, we should minimize it to be as small as possible. We found out, that the increasing of the number of phases brings about decreasing of the cogging forces. The minimization of the detent force reduces the vibrations of the PMLSM and provokes that the control system for the runner positioning can be straightforward.

The paper describes calculation of the dynamics characteristics using the field-circuit mathematical model of the 5-phase actuator. Using the FEM model, the nonlinear magnetic field analysis has been performed. Our field-circuit procedure has been implemented in

Matlab/Simulink computer package. The comparison of the calculation results by the proposed method and the findings of the experimental tests prove the correctness of the mathematical modeling.

2. Description of the linear motor

The schematic outline of the halved motor cross section is shown in Fig. 2. The internal radius of the mover and external radius of the stator as well as length of the motor are also given. The stator is assembled from five coils which are creating the five-phase excitation winding. Each coil of the PMTLM stator has been located in the stator segment of iron ferromagnetic core. The number of turns per phase is equal to $N = 280$. The segments are magnetically separated. The distance between each phase is adjusted to the pole-pitch τ_p . This way, the magnetic field creates the fluxes surrounding each phase of the stator. Configuration of the ferromagnetic core is characterized by the repeating of the stator-mover segments every 30 mm (two times in the pole-pitch τ_p).

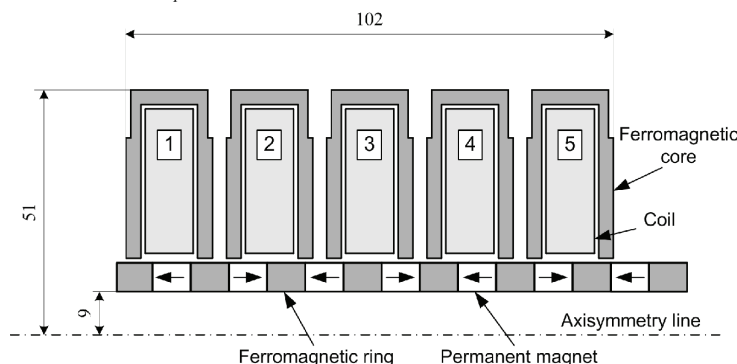


Fig. 2. Cross section with main dimensions of the 5-phase PMTLM

The mover (runner) parts consist of a multi-pole permanent magnet. It is assembled from ferromagnetic rings and magnets. The fields of the magnets, which are located on a non-ferromagnetic pipe, are separated from each other by the ferromagnetic parts (rings). Applying the 5-phase sinusoidal current excitation with the suitable shift, the synchronous work mode of the actuator is obtained. In this mode, the rated parameters of the motor are: current value $I_m = 8$ A, velocity of the mover $v_N = 1$ m/s and average force $F_N = 448$ N.

3. Mathematical model for the field-circuit analysis

The field model has been created with using the finite element method (FEM) [12]. The solver has been performed with the magnetic vector potential. The induced eddy currents were neglected in this field model. Taking into account the magnetic vector potential \vec{A} , we have solved the nonlinear Poisson's differential equation

$$\nabla \times \left(\frac{1}{\mu(B)} \nabla \times \bar{\mathbf{A}} \right) = \bar{\mathbf{J}}. \quad (1)$$

Including the cylindrical symmetry of the object (Fig. 1), we obtained the elliptic differential equation for the A_φ component of the vector potential. The nonlinear function $\mu(B)$ of the magnetic permeability has been included

$$\frac{\partial}{\partial r} \left(\frac{1}{\mu(B)} \frac{\partial A_\varphi}{\partial r} \right) + \frac{1}{r \cdot \mu(B)} \frac{\partial A_\varphi}{\partial r} + \frac{\partial}{\partial z} \left(\frac{1}{\mu(B)} \frac{\partial A_\varphi}{\partial z} \right) - \frac{1}{\mu(B)} \frac{A_\varphi}{r^2} = J_\varphi. \quad (2)$$

The magnetic flux density value was calculated from the knowledge of the A_φ component

$$\vec{B} = -\frac{\partial A_\varphi}{\partial z} \vec{1}_r + \frac{1}{r} \frac{\partial(r A_\varphi)}{\partial r} \vec{1}_z. \quad (3)$$

For the circuit model under assumed current excitation, we need only the magnetic force [13]. It has been obtained using the Maxwell's stress tensor

$$\vec{F}_e = \int_{\Omega} f d\Omega = \int_{\Gamma} \vec{T} \cdot d\vec{\Gamma}. \quad (4)$$

For the cylindrical system of coordinates, the H_r and H_z components, as well as H magnitude of magnetic intensity have been taken for calculating of the Maxwell's stress tensor components

$$\vec{T} = \begin{bmatrix} \mu(B) \left(H_r^2 - \frac{1}{2} H^2 \right) & \mu(B) H_r H_z \\ \mu(B) H_r H_z & \mu(B) \left(H_z^2 - \frac{1}{2} H^2 \right) \end{bmatrix}. \quad (5)$$

The field-circuit model has been obtained using the Lagrange's formulation [14, 15]. Due to the construction with separated magnetically segments, each phase can be modelled independently. In case of the current excitation, one generalized coordinate must be included for each segment only. It is the mover position z

$$\vec{q} = (z). \quad (6)$$

In the horizontal position of the motor any gravitational force should be taken into account. Thus, the potential energy U is equal to zero. The kinetic co-energy T is described according the formula below

$$T = \frac{1}{2} m \dot{z}^2, \quad (7)$$

where m is the mass of the mover, \dot{z} is time derivative of the displacement.

Using the Hamiltonian's principle [15], the Lagrange function of the system, defined as a difference between kinetic co-energy and potential energy, is equal to

$$L = T - U = \frac{1}{2} m \dot{z}^2. \quad (8)$$

From the Lagrange equation

$$\frac{\partial}{\partial t} \left(\frac{\partial L}{\partial \dot{z}} \right) - \frac{\partial L}{\partial z} = -D \dot{z}, \quad (9)$$

where D is the friction coefficient, we obtained two differential equations of first order, both for the mechanical part of the system, only

$$\frac{dv}{dt} = \frac{F(i, z) - Dv}{m}, \quad \frac{dz}{dt} = v. \quad (10)$$

The equation set above has been implemented in Matlab/Simulink software platform (Fig. 3). The function $F(i, z)$, obtained by the field calculations, has been implemented as a look-up table for each phase independently. The cogging force has been calculated separately, assuming no current excitation.

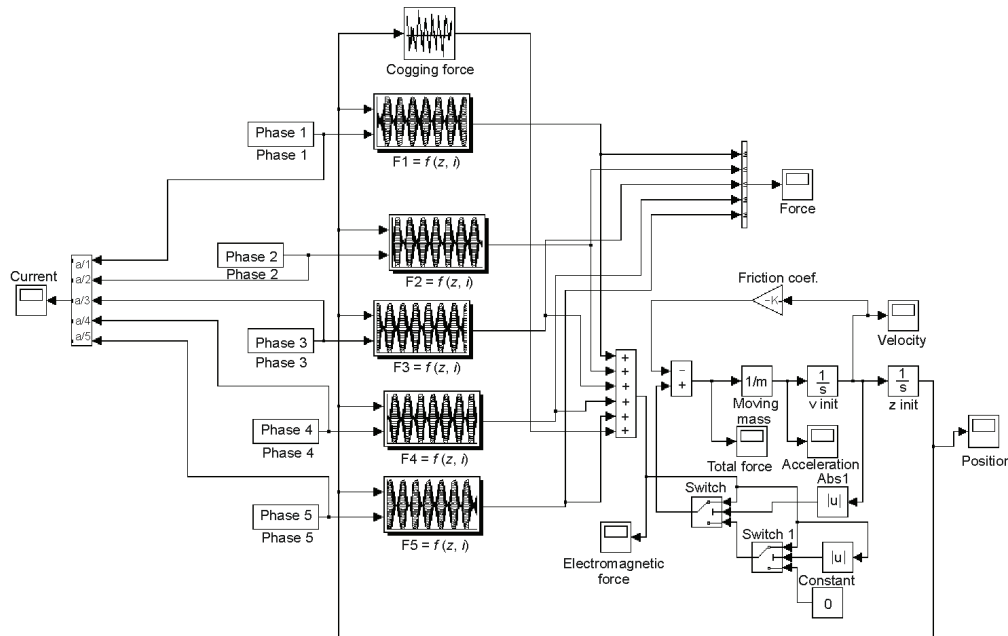


Fig. 3. The field-circuit mathematical model of the 5-phase PMTLM

4. Calculation results and measurement verification

The calculations have been carried out for the 5-phase supplying. The current excitation has been implemented using the PWM converter. The simulations and measurements of the mover position (vs. time) for different established values of velocity and different values of

the runner load have been simulated (Figs. 4-9). In all cases the nominal current value ($I_m = 8$ A) has been assumed.

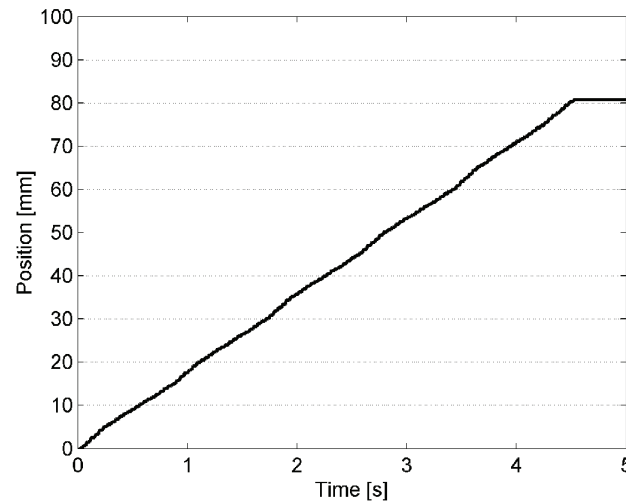


Fig. 4. The calculated dynamic characteristic of the mover position under no-load state for the average velocity $v = 18$ mm/s

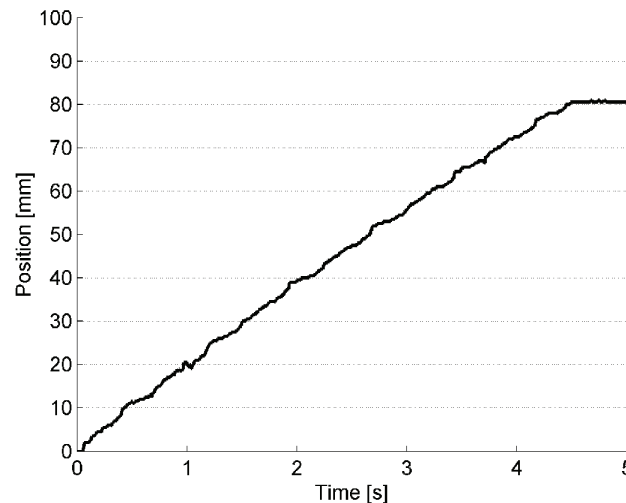


Fig. 5. The measured wave of the mover position for the average velocity $v = 18$ mm/s.
No-load condition

In figures 4 and 5 very low speed of the mover ($v = 18$ mm/s), was assumed under the no-load state. There are some differences between the calculated and measured waves. From the simulations we have obtained the smoother waves than those from experiments. The small oscillations of the runner position are visible. It is due to the assumptions in the mathematical

modeling, and the friction force values randomize, especially. However, the average velocities of the runner movement are quite close. According increasing of the average value of the mover velocity, the mover position waves differ each other (Figs. 4 and 6). In case of the nominal velocity ($v = 1 \text{ m/s}$) the inertia and friction of the mover strongly influences its position wave (Figs. 6 and 7). At the first moment of the movement, the small oscillations are visible. The oscillations vanish after 0.6 s. The measured and calculated waves are similar, which confirms the usefulness of the mathematical model.

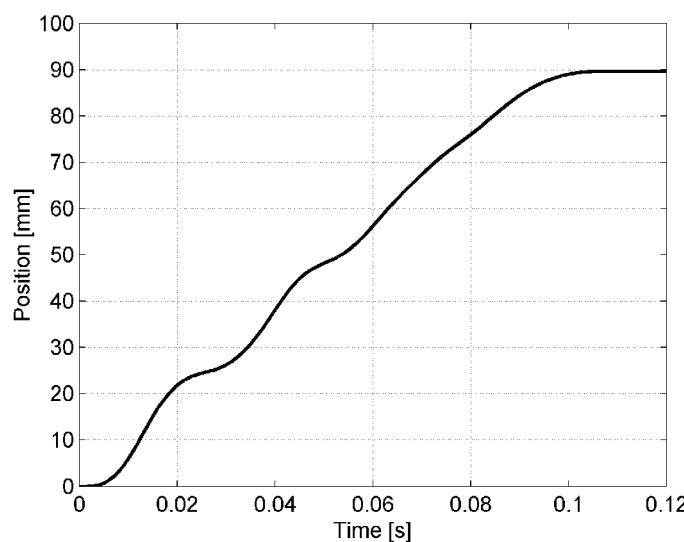


Fig. 6. The calculated wave of the mover position for the nominal velocity (no-load conditions)

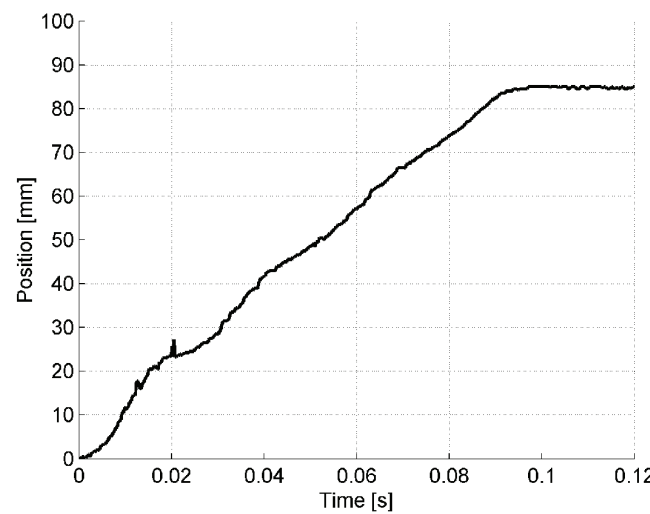


Fig. 7. The measured mover position vs. time for the nominal velocity (no-load conditions)

The motor could be linked with different loads. In our case, we have used an inertia load. It was a loaded cart, which was placed on the sliding linear bearings. The additional mass of $m = 19.2$ kg was linked with the mover. We have assumed a relative low velocity $v = 5$ cm/s. The moving mass increase causes the additional ripples in the mover position wave (Figs. 8 and 9). It is visible both in measured and calculated transients of the runner. It is mainly due to the actuator thrust ripples.

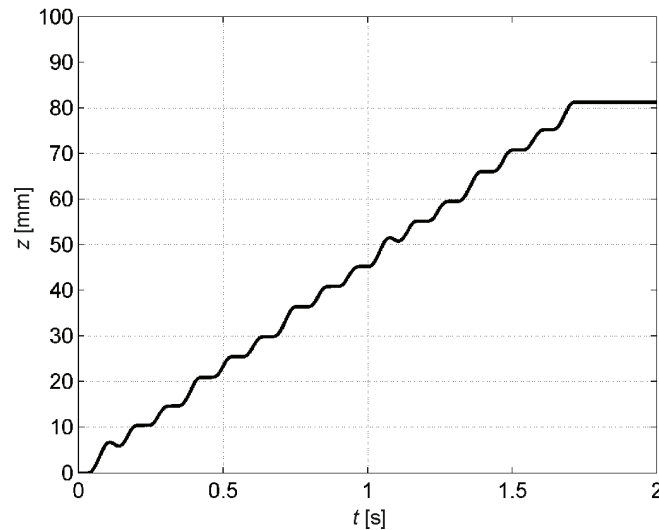


Fig. 8. The calculated wave of the mover position for the average velocity $v = 50$ mm/s and under the additional inertial force concerned with the joined mass of $m = 19.2$ kg

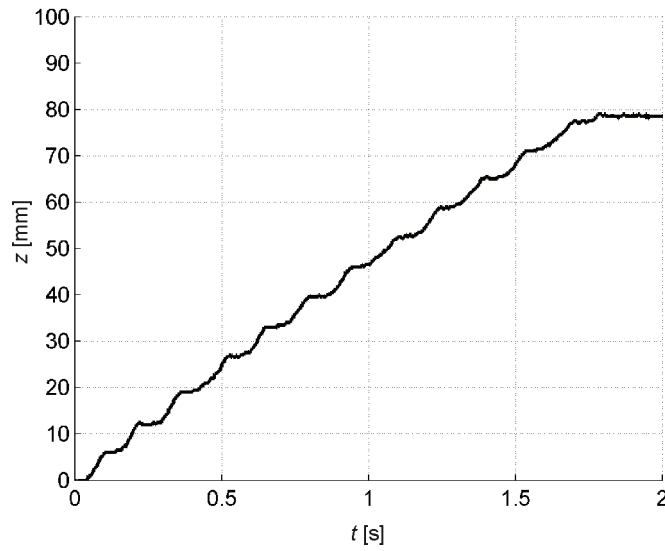


Fig. 9. The measured mover position vs. time for the average velocity $v = 5$ cm/s and under the additional inertial force concerned with the joined mass of $m = 19.2$ kg

5. Conclusions

In the paper, the field-circuit model for calculating of the dynamic characteristics is presented. The 5-phase permanent magnet tubular linear motor (PMTLM) has been considered. The calculated and tested results were compared. Due to the simplifications in the mathematical modelling and the errors of the experimental results the small local discrepancies are visible in the obtained waves. Under the no-load conditions and for relatively slow velocity, there are only low oscillations in the mover position wave. Due to mover inertia, increasing of the velocity causes higher oscillations of the mover position. Under load conditions, the position ripples appears. However, the effects (oscillations and ripples) occur in both mathematical model and measurement test. Although the sinusoidal current excitation has been considered in the paper, the other current supplying is possible to apply for the modelling. The extended field-circuit model can be used for the voltage supplying as well. The presented mathematical model can be used in the numerical simulations of the complex drive system operation with the PMTLM. It is possible to implement many control algorithms in the presented calculation model. It is very convenient in the design process of the drive system or servo application.

Acknowledgements

This work was partially supported by the NCBiR (National Centre for Research and Development, Poland) under grant No N R01 0026 04

References

- [1] Eastham J.F., Profumo F., Teneoni A., Gianolio G., *Linear drive in industrial application: state of the art and open problems*. Paper presented at the XV International Conference on Electrical Machines (ICEM), 25-28 August, Brugge, Belgium, available as paper 620 (2002).
- [2] Tomczuk B., Waindok A., *Linear motors in mechatronics – achievements and open problems. Monograph: Transfer of innovation to the interdisciplinary teaching of mechatronics for the advanced technology needs*. Opole University of Technology, OWPO, Opole: 343-360 (2009).
- [3] Gordon S., Hillery M.T., *Development of a high-speed CNC cutting machine using linear motors*. Journal of Materials Processing Technology 166: 321-329 (2005).
- [4] Tomczuk B., Waindok A., *Tubular Linear Actuator as a Part of Mechatronic System*, proceedings of the 4th International Conference Mechatronic Systems And Materials (MSM 2008), 14-17 July, Białystok: 64-65 (2008).
- [5] Zhu Y.-W., Lee S.-G., Chung K.-S., Cho Y.-H., *Investigation of auxiliary poles design criteria on reduction of end effect of detent force for PMLSM*. IEEE Trans. on Magnetics 45(6): 2863-2866 (2009).
- [6] Boldea I., Nasar S.A., *Linear electric actuators and generators*. Cambridge Univ. Press, New York, USA. (2005).
- [7] Sheikh-Ghalavand B., Vaez-Zadeh S., Hassanpour Isfahani A. *An improved magnetic equivalent circuit model for iron-core linear permanent-magnet synchronous motors*. IEEE Trans. on Magnetics 46(1): 112-120 (2010).
- [8] Kim W.-J., Murphy B.C., *Development of a novel direct-drive tubular linear brushless permanent-magnet motor*. International Journal of Control, Automation and Systems 2(3): 279-288 (2004).
- [9] Tomeczuk B., Schröder G., Waindok A., *Finite element analysis of the magnetic field and electromechanical parameters calculation for a slotted permanent magnet tubular linear motor*. IEEE Trans. on Magnetics 43(7): 3229-3236 (2007).

- [10] Faiz J., Ebrahimi-Salari M., Shahgholian Gh., *Reduction of cogging force in linear permanent-magnet generators*. IEEE Trans. on Magnetics 46(1): 135-140 (2010).
- [11] Tomczuk B., Waïndok A., *The multiphase tubular linear motor*. Patent No P 381987 (2010).
- [12] Meeker D., *FEMM 4.0, User's Guide*. Univ. of Virginia, Virginia (2004).
- [13] Tomczuk B., Waïndok A., *Integral parameters of the magnetic field in the permanent magnet linear motor*. Monograph entitled *Intelligent Computer Techniques in Applied Electromagnetics* (in series *Studies in Computational Intelligence*). Springer Verlag, Heidelberg, Germany 119: 277-281 (2008).
- [14] Tomczuk B., Sobol M., *Analysis of tubular linear reluctance motor (TLRM) under various voltage supplying*. Paper presented at the XVI International Conference on Electrical Machines (ICEM), 5-8 September, Cracow, Poland, available as paper 792 (2004).
- [15] Tomczuk B., Sobol M., *A Field-Network model of a linear oscillating motor and its dynamics characteristics*. IEEE Trans. on Magnetics 41(8): 2362-2367 (2005).